Journal of Petroleum Exploration and Production Technology (2023) 13:1951–1962
https://doi.org/10.1007/s13202-023-01654-x

ORIGINAL PAPER-PRODUCTION ENGINEERING

A novel analytical technique for determining inflow control devices flow area in CO_2-EOR and CCUS projects

Hamed Rezvani[1] · **Yousef Rafiei**[1]

Received: 26 July 2022 / Accepted: 19 May 2023 / Published online: 3 June 2023

Abstract

CO_2-EOR is one of the principal techniques for enhanced oil recovery (EOR). The CO_2 injection not only promotes oil recovery but also leads to greenhouse gas discharge reduction. Nonetheless, a key challenge in the CO_2 flooding process is a premature CO_2 breakthrough from highly permeable zones. In recent years, Inflow Control Devices, ICDs, have been used as a potential solution to mitigate an early gas breakthrough. The key and important parameter in ICDs installation is obtaining its opening flow area. The common ways to obtain the ICD flow area such as utilizing optimization algorithms are very complicated and time-consuming, and further these methods are not analytical. The aim of this work is to solve the mentioned challenges—postpone the breakthrough time in gas injection and present an easy, fast, and analytical technique for obtaining ICDs flow area. This paper presents a new analytical method for obtaining inflow control devices flow area for injection wells in an oil reservoir under CO_2-EOR in order to balance the injected CO_2 front movement in all layers. Then, in order to compare the advantages and disadvantages of the presented technique with other methods such as optimization algorithms, a case study has been done on a real reservoir model under CO_2 injection. Later, the results of studied scenarios in the case studied are given and compared. The results show that by utilizing the proposed method recovery factor is raised by improving sweep efficiency, and the breakthrough time is more postponed compared to the other methods about 400 days. Further, the ICD flow area calculation takes 2 min by presented analytical techniques, but the optimization algorithm takes 4040 min to run the simulation model to find the ICD flow area. In the end, the findings of the presented analytical formula can help to set the ICD flow area very fast without the simulation and help researchers for a better quantitative understanding of parameters affecting the ICD flow area by the given formula such as reservoir permeability.

Keywords CO_2-EOR · Inflow control devices · Breakthrough time

List of symbols

A	Flow area (ft^2)
A_c	Inflow control device flow area (ft^2)
C_v	Inflow control device constant
D	Diameter (ft)
f	Fanning friction factor
h	Thickness (ft)
k	Permeability (mD)
P_{wi}	Injection pressure at sand face (Psia)
P_{bh}	Bottom hole pressure (Psia)
P_e	Reservoir pressure (Psia)
Q_g	Gas production rate (Scf/day)
Q_o	Oil production rate (Bbl/day)
q_{inj}	Injection rate (Scf/day)
r_e	Reservoir radius (ft)
r_w	Well radius (ft)
S	Skin factor
V	Velocity (ft/s)
Z	Compressibility factor
Δ	Delta
π	Mathematical constant
μ	Viscosity (Cp)

Acronyms

API	American petroleum institute
CCUS	Carbon capture, utilization, and storage
CO_2	Carbon dioxide
Cp	Centi poise
EOR	Enhanced oil recovery
ft	Foot
ICD	Inflow control device
ICV	Inflow control valve

✉ Yousef Rafiei
y.rafiei@aut.ac.ir

[1] Department of Petroleum Engineering, Amirkabir University of Technology, Tehran, Iran

mD	Millidarcy
NPV	Net present value
Psia	Pounds per square inch absolute
Scf	Standard cubic foot
STB	Stock Tank Barrel

Introduction

CO_2-EOR mechanism

The CO_2 injection into oil reservoirs is a commonly used approach for carbon capture, utilization, and storage (CCUS) projects in order to reduce greenhouse gases and enhanced oil recovery. CO_2 injection efficiency is reliant on CO_2 miscibility in oil (Zhang et al. 2018). In an oil reservoir containing a significant amount of light hydrocarbons during the injection of CO_2, the oil light hydrocarbons dissolve within the CO_2, and CO_2 dissolves in the oil. Therefore, the oil viscosity reduces significantly (Zhang et al. 2015).

Oil viscosity reduction causes an improvement in oil mobility, which decrease the residual oil saturation in the reservoir and enhanced oil recovery(Li et al. 2013). The CO_2 dissolution in oil at specific reservoir conditions such as oil compositions, temperature, and pressure, provokes the oil to swell, which plays an essential role in attaining better oil recovery. Swelled oil droplets force oils—initially unable to produce—to get out of the pores and swipe toward the production well. Therefore, the residual oil saturation decreases (Perera et al. 2016).

CO_2-EOR challenges

Although the injection of CO_2 reduces greenhouse gases and increases oil recovery, it is typically utilized in carbonate reservoirs, which usually have low permeability. However, the reservoirs usually include zones with high permeability (Siqueira et al. 2017) and fractures in reservoir layers (Dejam andHassanzadeh 2018b). Therefore, utilizing CO_2 injection in EOR projects have significant problems and challenges with CO_2 short-circuiting between injection and production wells and the early breakthrough of CO_2 in high permeable, thief zones, and aquifer (Dejam and Hassanzadeh 2018a). Hence, injected CO_2 production prevents oil production from the remaining layers, and significant volumes of oil will remain in the reservoir(Yang et al. 2019). Thus, having a well-balanced injected CO_2 influx is required to maximize oil production.

Controlling CO_2 injection in the high permeable and thief zones, breakthrough layers, where the CO_2 early production happens, yields a better CO_2 distribution in the reservoir, which improves the oil recovery(Yu et al. 2014). To manage the breakthrough time in reservoirs is required to control each layer individually in the well; therefore, advanced completion with inflow control devices can be employed (Mohammadpourmarzbali et al. 2019).

Inflow control device

Inflow Control Devices are a conventional type of advanced completions that present passive inflow control. ICDs are broadly utilized and can be a perfected well completion technology (Ugwu and Moldestad 2018). Inflow Control Devices have been utilized to balance the injected fluid influx by making extra backpressure in the layers produce excess fluid at tremendous rates (Ratterman et al. 2005). Employing ICDs can delay CO_2 breakthroughs and maintain a balanced flow. The ICDs have to be designed based on the reservoir properties (Rahimbakhsh and Rafiei 2018) to manage CO_2 flow and make a better CO_2 distribution in the reservoirs, providing high-quality CO_2 storage in the reservoir during the oil production time.

Brouwer et al. (2001) managed the injected fluid in a high-degree heterogeneous field with a horizontal injection well by using control valves to prevent injection fluid breakthrough and maximize recovery by a simple algorithm in two scenarios, constant flow scenario and constant pressure scenario (Brouwer et al. 2001). Brouwer et al. (2004) developed a closed-loop method to optimize the flooding process by maximizing the net present value (NPV) (Brouwer et al. 2004). Naus et al. (2004) formed an operational approach for commingled production with infinitely changeable ICV using sequential linear programming for short-term production optimization (Naus et al. 2004). Alhuthali et al. (2010) proposed a rate control technique for optimizing water flood in an intelligent well containing ICVs (Alhuthali et al. 2010). Essen et al. (2010) propose a workflow based on a gradient-based optimization technique in order to predict the production and injection rate of inflow control valves in horizontal wells (Van Essen et al. 2010). Hassanabadi et al. (2012) adjusted the ICD flow area by using particle swarm optimization and the neural smart system to maximize the cumulative oil production and minimize cumulative water production. In this study, the algorithm has been implemented separately for all valves (Hassanabadi et al. 2012). Fonseca et al. (2015) studied ensemble multi-objective production optimization of on–off inflow control devices on a real-field case by a modified net present value (Fonseca et al. 2015). Chen and Reynolds (2017) optimize ICV settings and well controls concurrently to maximize NPV. In this study, the NPV achieved by this method was compared with two other scenarios NPVs, NPV achieved by only well control optimization, and NPV achieved by only ICV settings optimization (Chen and Reynolds 2017). In 2018, Aakre investigated the performance of the autonomous inflow control valves in injecting CO_2 into the reservoir. This is the first time in the world that autonomous inflow control valves are used in CO_2—EOR operations (Aakre et al. 2018). Cao et al. (2019) presented a novel well fluid modeling for heterogeneous reservoirs in order to accurate the simulation result (Cao et al. 2019). Salvesen et al. (2020) simulated CO2-EOR utilizing the OLGA in combination with ROCX by employing autonomous inflow control valves in wells (Salvesen Holte et al. 2020). Safaei presented a new method in order to accurate CO2 and brine interfacial tension modeling (Safaei-Farouji et al. 2022b) and investigated the CO2 trapping via machine learning (Safaei-Farouji et al. 2022a) to improve and enhance CO2 storage efficiency in underground reservoirs.

Literature review on the CO_2-EOR and use of ICDs in the CO_2 injection process reveals that the CO_2 short cycle and premature breakthrough time is an essential problem that can be mitigated by inflow control devices. Furthermore, an important question is what will be the required flow area of the ICDs in order to control fluid injection or production in different layers in which most of the techniques are based on optimization algorithms. To do so, a reliable system model is required which is not available most of the time. In addition, solving optimization algorithms for reservoirs with many wells and complex system models is very time-consuming. Likewise, there is not much effort to develop analytical techniques to calculate injected fluid rate and flow area at the same time in order to obtain ICDs flow area only by using properties of the system independent of the system's complex structure. In other words, previously performed studies were not based on an analytical formula; hence, the investigation and effect of parameters such as reservoir parameters were difficult. As a result, the current research represents a novel analytical technique to calculate injected CO2 rate and flow area in order to maximize breakthrough time and improve oil production.

This research presents a new analytical formula for obtaining the ICDs flow area. First, the design and simulation section is given in which the new formula is derived. Then, scenarios are defined in order to compare the advantages and disadvantages of the proposed methods with other methods. Finally, the results section is presented.

Design and simulation

This study initially aims to develop a new analytical technique to determine the ICDs flow area in order to balance the gasfront movement in reservoir layers with different permeability to maximize breakthrough time. In this method, at first in the part 1, by utilizing a fluid flow equation in porous media, an equation is developed in which the gasfront velocity in a high permeable layer reduces to the gas front velocity of the injected gas in a low permeable layer. Second in the part 2 and part 3, this equation is combined by 2 different equations which are calculated pressure drop due to the ICD. Finally, by considering these 3 equations, the analytical technique is developed for calculating the ICD flow area in which gasfront moves by the same velocity in low and high permeable layers.

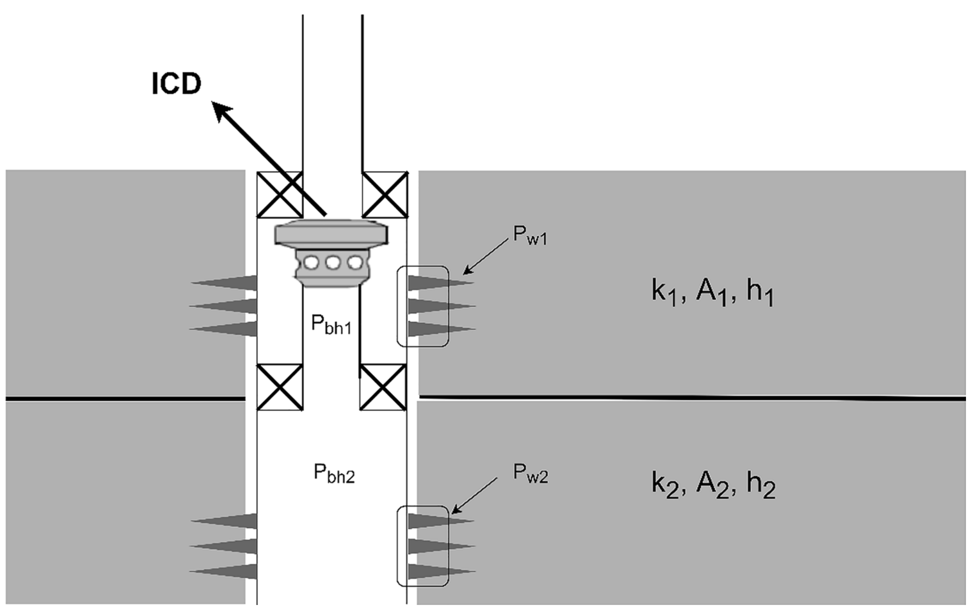

Fig. 1 Scheme of a two-layer reservoir employing ICD in layer 1

New analytical method

Part 1

Assuming a reservoir with 2 layers each having (Fig. 1) different permeability and thickness, the ICD will set up at a high permeable layer (layer 1 in this example). The injection inflow equation (for CO_2 gas injection) from the well to the reservoir for each layer is as follows; assumed that injection is a piston-like gas flooding, constant reservoir properties during the injection periods, the injection well is a vertical well, and steady-state flow (Fetkovich 1975):

$$q_i = \frac{k_i h_i}{1422 \times \overline{\mu z} \times \left[\ln \frac{r_e}{r_w} - 0.75 + s_i'\right]} \left(p_{w_i}^2 - p_e^2\right) \tag{1}$$

where q_i is the injection rate in layer i; h_i and K_i are the thickness and permeability of layer i respectively;s_i' is the sum of total Darcy skin and non-Darcy flow skin of layer i; μ is CO_2 viscosity; P_e is reservoir pressure; and P_{wi} is CO_2 injection pressure at sand face for layer i.

Front fluid flow velocity for each layer can be obtained dividing the flow rate (Eq. 1) by the cross-section area for each layer:

$$v_i = \frac{1}{A_i}\left[\frac{k_i h_i}{1422 \times \overline{\mu z} \times \left[\ln \frac{r_e}{r_w} - 0.75 + s_i'\right]} \left(p_{w_i}^2 - p_e^2\right)\right] \tag{2}$$

$$A_i = 2\pi r_i h_i \tag{3}$$

where V_i is the front velocity in layer i, and r_i is the injected CO_2 front radius from the injection well in layer i (Fig. 2).

In order to delay the CO_2 breakthrough time in a layer with higher permeability, the CO_2 front velocity in the high permeable layer should reduce to the CO_2 front velocity in the low permeable layer in order to make the CO_2 front in each layer reach the production well at the same time. Hence, the front velocity in each layer should be equal (Eq. 4), this means that the front radius at each time in both layers is the same (Eq. 5).

$$V_1 = V_2 \tag{4}$$

$$r_1 = r_2 \tag{5}$$

By substituting Eq. (2) in Eq. (4):

$$\frac{k_1 h_1}{\left[\ln \frac{r_e}{r_w} - 0.75 + s_1'\right]} \frac{1}{A_1}\left(p_{w_1}^2 - p_e^2\right) = \frac{k_2 h_2}{\left[\ln \frac{r_e}{r_w} - 0.75 + s_2'\right]} \frac{1}{A_2}\left(p_{w_2}^2 - p_e^2\right) \tag{6}$$

where P_{w2} is sand face pressure for layer 2 which is equal to P_{bh2} (as there is no ICD in layer 2), and P_{w1} is ICD outlet pressure, or sand face pressure, in layer 1.

Since it is important to know P_{w1}, by solving Eq. (6) for P_{w1}:

$$p_{w_1}^2 = \frac{k_2 h_2}{k_1 h_1} \frac{A_1}{A_2} \frac{\left[\ln \frac{r_e}{r_w} - 0.75 + s_1'\right]}{\left[\ln \frac{r_e}{r_w} - 0.75 + s_2'\right]} \left(p_{w_2}^2 - p_e^2\right) + p_e^2 \tag{7}$$

To obtain the cross-section area in Eq. (7) which is unknown, Eqs. (3) and (5) is combined to obtain the cross-section:

$$\frac{A_1}{A_2} = \frac{2\pi r_1 h_1}{2\pi r_2 h_2} = \frac{h_1}{h_2} \tag{8}$$

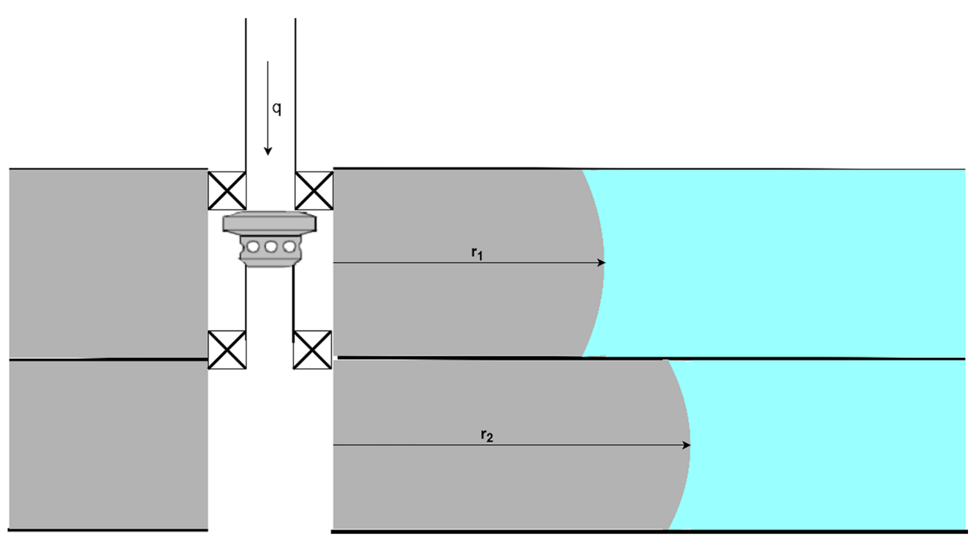

Fig. 2 Injected gas front radius in a two-layer reservoir

Now, Eq. (7) can be re-write in order to eliminate the cross-section:

$$p_{w_1}^2 = \frac{k_2}{k_1} \frac{\left[\ln \frac{r_e}{r_w} - 0.75 + s_1'\right]}{\left[\ln \frac{r_e}{r_w} - 0.75 + s_2'\right]} \left(p_{w_2}^2 - p_e^2\right) + p_e^2 \tag{9}$$

Part 2

As shown in Fig. 3, the pressure loss across the ICD is as follows.

$$\Delta P_{ICD} = p_{bh_1} - p_{w_1} \tag{10}$$

where P_{bh1} is bottom hole injected pressure in layer 1, and P_{w1} is ICD outlet pressure in layer 1 calculated from Eq. (9), so:

$$\Delta P_{ICD} = p_{bh_1} - \sqrt{\frac{k_2}{k_1} \frac{\left[\ln \frac{r_e}{r_w} - 0.75 + s_1'\right]}{\left[\ln \frac{r_e}{r_w} - 0.75 + s_2'\right]} \left(p_{w_2}^2 - p_e^2\right) + p_e^2} \tag{11}$$

Part 3

Also, the pressure loss equation for ICD is as follows (GeoQuest 2014):

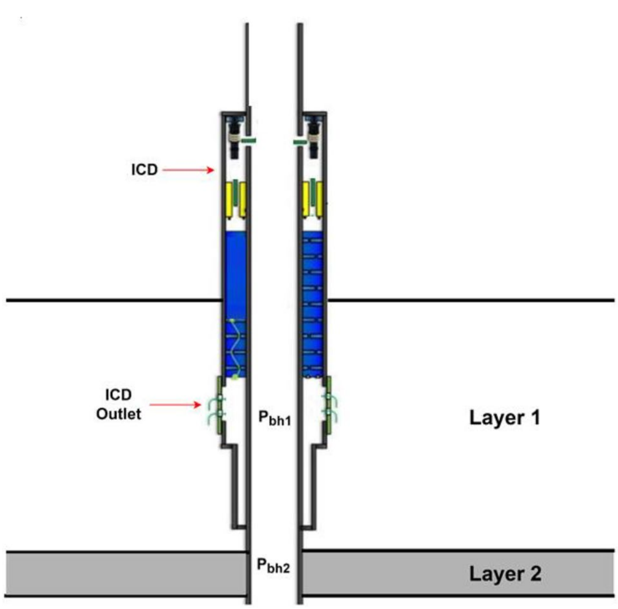

Fig. 3 Pressure drop in an ICD

$$\Delta P_{ICD} = C_u' \frac{\rho\left(\frac{q_{ICD}}{A_c}\right)^2}{2C_v^2} + 2C_u' f \frac{L}{D} \rho \left(\frac{q}{A_p}\right)^2 \tag{12}$$

where C_u' is unit constant, C_v is ICD constant, A_c is the ICD cross-section, A_p is the well cross-section, D is well diameter, f is the Fanning friction factor, and ρ is the fluid density.

By the combination of Eqs. (11) and (12):

$$C_u' \frac{\rho q_{ICD}^2}{2C_v^2 A_c^2} + 2C_u' f \frac{L\rho q^2}{DA_p^2} = p_{bh_1} - \sqrt{\frac{k_2}{k_1} \frac{\left[\ln \frac{r_e}{r_w} - 0.75 + s_1'\right]}{\left[\ln \frac{r_e}{r_w} - 0.75 + s_2'\right]} \left(p_{w_2}^2 - p_e^2\right) + p_e^2} \tag{13}$$

By solving Eq. (13) for A_c:

$$A_c = \sqrt{\frac{\frac{C_u' \rho q_{ICD}^2}{2C_v^2}}{p_{bh_1} - \sqrt{\frac{k_2}{k_1} \frac{\left[\ln \frac{r_e}{r_w} - 0.75 + s_1'\right]}{\left[\ln \frac{r_e}{r_w} - 0.75 + s_2'\right]} \left(p_{w_2}^2 - p_e^2\right) + p_e^2} - 2C_u' f \frac{L\rho q^2}{DA_p^2}}} \tag{14}$$

For simplifying the above equation:

$$A_c = \sqrt{\frac{D}{p_{bh_1} - B - C}} \tag{15}$$

where:

$$B = \sqrt{\frac{k_2}{k_1} \frac{\left[\ln \frac{r_e}{r_w} - 0.75 + s_1'\right]}{\left[\ln \frac{r_e}{r_w} - 0.75 + s_2'\right]} \left(p_{w_2}^2 - p_e^2\right) + p_e^2} \tag{16}$$

$$D = \frac{C_u' \rho q_{ICD}^2}{2C_v^2} \tag{17}$$

$$C = 2C_u' f \frac{L\rho q^2}{DA_p^2} \tag{18}$$

where B can represent sandface pressure, D can represent acceleration term, and C can represent friction term.

To maximize the CO_2 breakthrough time, the ICDs flow area can be adjusted according to Eq. (15) in which the CO_2 front moves in the high permeable layer at the same velocity as in the low permeable layer.

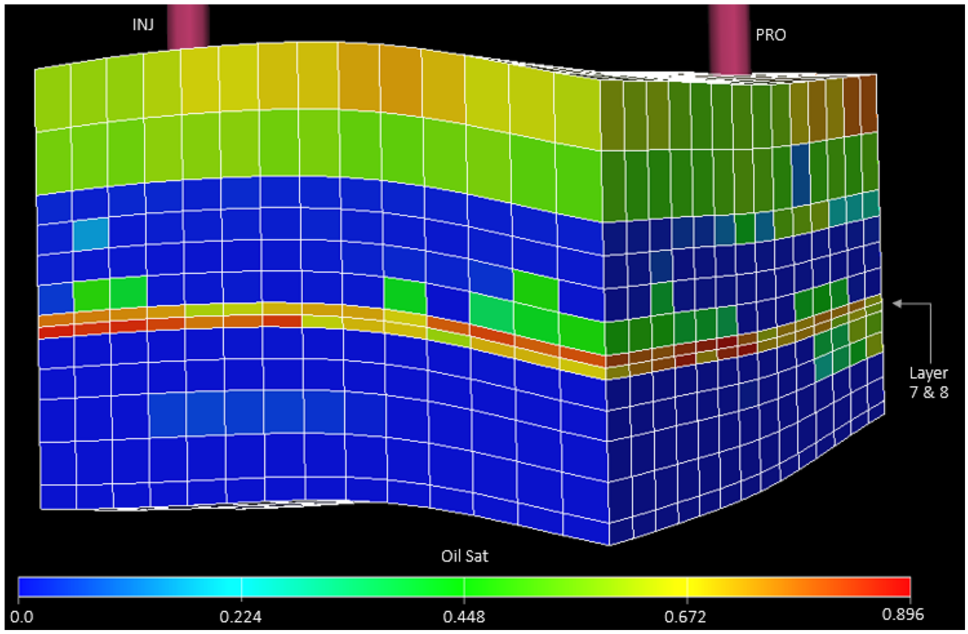

Fig. 4 Reservoir model in this study (colours representing oil saturation)

Table 1 Properties of the studied reservoir model

Dimension (ft^3)	Depth (ft)	Pressure (Psia)	Temperature (°C)	Average permeability (mD)	Average Porosity (%)
6561 × 6561 × 250	6400	4700	93	Layer 7 = 400 Layer 8 = 800	25

Table 2 Reservoir fluid properties

Bubble point pressure	1000 psia
API	21
Minimum miscibility pressure for CO_2	2740 Psia
Temperature	93 °C

Case study

In order to compare the advantages and disadvantages of the proposed method to other methods, four scenarios have been studied in this research. At first, a base scenario is defined. Then two scenarios are defined with ICD installation in a high permeable layer—in these two scenarios, the ICD flow area is calculated with the optimization algorithm and the proposed method, respectively. Finally, the sensitivity analysis is done on the ICD flow area. And, the results of all scenarios are compared in the result section. It should be noted that in all scenarios initial condition, reservoir property, injection rate, and production rate are the same—only the ICD flow area is different.

Table 3 Production and injection well condition

Production well	Injection well
Well head pressure = 250 psia	CO_2 injection rate = 6000 Mscf/day

The reservoir model under this study for all scenarios consists of 1 producer and 1 injector. It has 2 appropriate reservoir layers for CO_2 injection (layers 7 and 8).

The location of the wells has been shown in Fig. 4, and the properties of the reservoir are given in Table 1. Reservoir fluid is heavy oil (Table 2) and is suitable for CO2 flooding. Furthermore, For the simulation of the CO_2 injection, the compositional simulator is utilized.

Base scenario

In this scenario, the production well was producing with constant wellhead pressure, and constant CO_2 injected rate at the injection well as shown in Table 3.

Optimization algorithm

Numerous algorithms which are classified into three classes, including approximate, exact, or heuristic/metaheuristic, are utilized to determine the optimal solutions. During the past decade, optimization problems have been resolved by metaheuristic algorithms.

GWO is a recently advised swarm-based metaheuristic. It was developed and suggested by Mirjalili (Mirjalili et al.

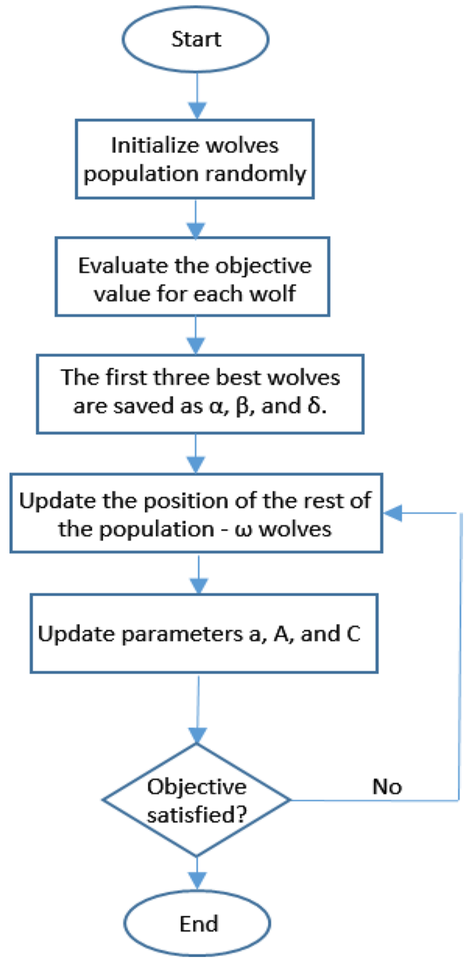

Fig. 5 The general steps of the GWO algorithm

Table 4 Calculated ICDs flow area using GWO

ICDs flow area	ft^2
A_c	0.0005788

2014). It is stimulated by the hunting behavior and leadership of grey wolves in the environment. The population is classified into four types, including alpha (α), beta (β), delta (δ), and omega (ω) in this algorithm. The three most appropriate wolves are recognized as alpha, beta, and delta leading other wolves, or omega to the suitable search space areas. The wolves update their locations around alpha, beta, or delta during optimization (Amar et al. 2018). Also, the GWO algorithm's general steps are shown in Fig. 5:

The objective function was maximizing the NPV (which can be expressed by Eq. 19) by changing the ICD flow area. In this scenario, the injection and production conditions were the same as the base scenario (Table 3), and *GOW* is used to find the optimum ICD flow area. The determined values of the ICDs flow area can be seen in Table 4.

Table 5 Equation 15 parameters

ρ	45.88	lb/ft^3
p_{bh_1}	4805	Psia
p_{w_2}	4800	Psia
f	0.0015	
L	0.5	ft
D	0.58	ft
A_p	1.056	ft^2
C'_u	2.89E-14	

Table 6 Calculated ICDs flow area using the proposed method

ICDs flow area	ft^2
A_c	0.000472

$$NPV = \sum_{K=1}^{M} \frac{Q_o r_o - Q_w r_w - Q_g r_g - Q_i r_i}{(1+b)^{t_k}} - C_0 \tag{19}$$

where Q_o, Q_w, and Q_g are the oil, water, and gas production rate respectively; Q_i denotes the gas injection rate; r_o is the oil price; r_w and r_g are the cost due to the water and gas handling respectively; r_i is the injected gas cost; b is the annual discount rate, and C_o is constant cost.

Proposed method

In this scenario injection and production scenario was the same as the base scenario (Table 3), but ICD has been used in the high permeable layer (layer 8). Then, the developed analytical technique is employed to obtain the ICDs flow area.

The CO_2 injection rate in Table 3 and the Parameters in Table 5 have been used to calculate the ICDs flow area using Eq. (15). The determined values of the ICDs flow area can be seen in Table 6.

Further investigation

For further and better investigation and analysis, a variety of different ICD flow areas, including 0.00001, 0.0001, 0.0002, 0.0003, 0.0004, 0.0007, 0.001, and 0.005 ft^2 have been used in high permeable layer (layer 8). In these scenarios, injection and production conditions were the same as in the base scenario (Table 3).

Result and discussion

Figure 6 compares the CO_2 injection profile between both layers—high and low permeable layers—in all scenarios at the same time interval (after 9 years of injection). The

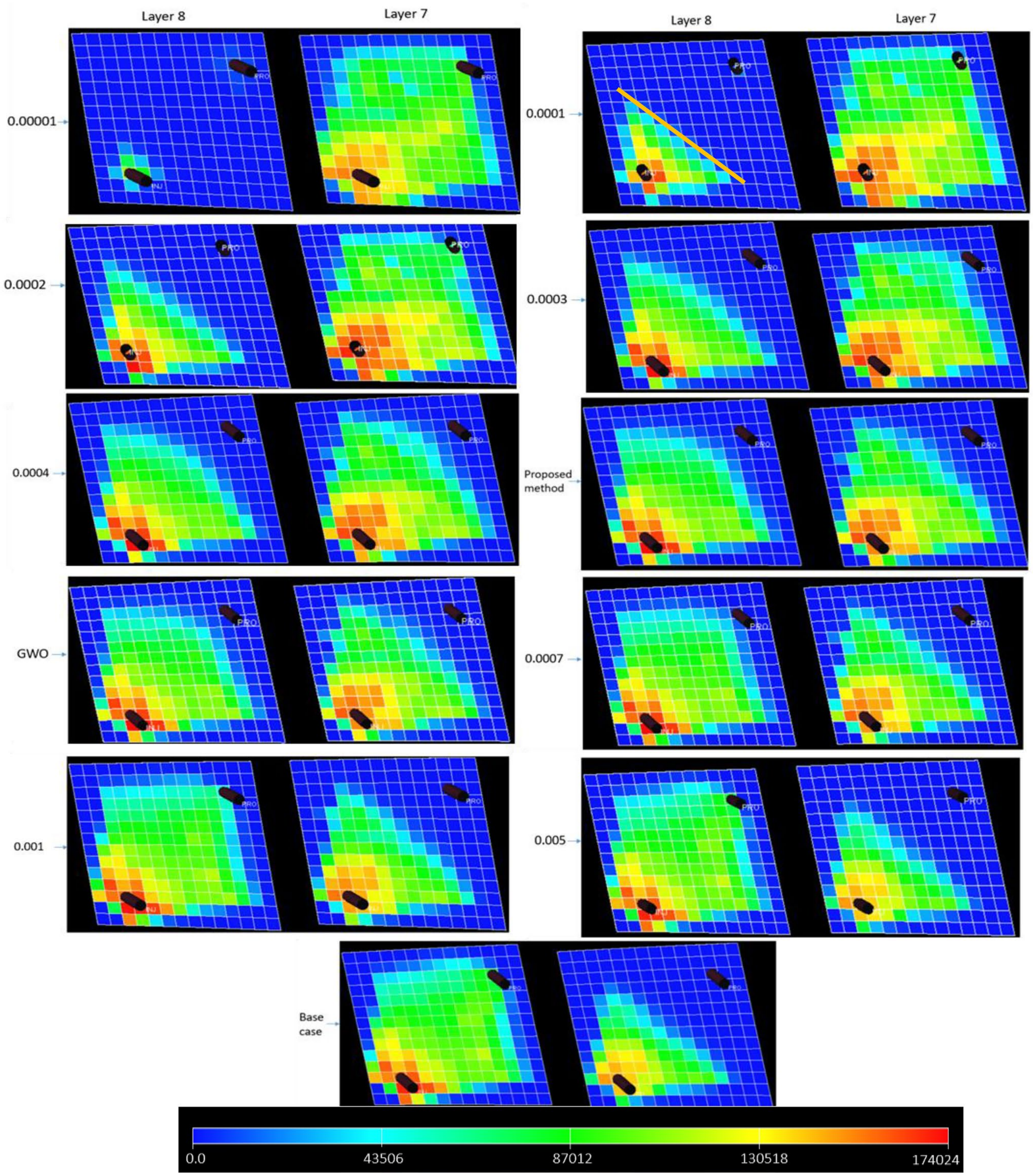

Fig. 6 Comparison of CO_2 front radius for all scenarios after 9 years of injection in layers 7 and 8 (colours representing CO_2 Fluid-in-place)

proposed analytical method has been able to balance the velocity of the fluid front in each of the two layers, and CO_2 breakthrough time in layers 8 and 7 happens at the same time. In fact, the proposed method was able to balance the injection fluid distribution in both layers by reducing the injection flow in the high permeability layer and increasing the injection flow in the low permeability layer. It means that more oil was displaced toward the production well in layer 7 and left less oil behind in layer 8. So, sweep efficiency was improved, and more oil was produced. Meanwhile, in other scenarios, the short-circuiting of CO_2 between injection and production wells happens. In other words, CO_2 cannot be stored in the reservoir for the CCUS and EOR applications. For instance, to clarify and illuminate the CO_2 breakthrough, consider the distribution of injected CO_2 in a scenario with $Ac = 0.0001\ ft^2$. The orange line, as shown in the top-right subplot, represents the injected CO_2 front, where the CO_2 fluid-in-place value suddenly drops to zero. As can be seen, injected CO_2 front reached the production well and moved much faster in layer 7 compared to layer 8, and CO_2 breakthrough happened.

As can be seen in Fig. 7, before breakthrough time, cumulative oil production at the base scenario and other scenarios are a bit higher compared to the proposed method scenario. On the other hand, after the CO_2 breakthrough time, it can be seen that more cumulative oil is produced in the proposed analytical method. In other words, although at the beginning other scenarios apparently worked better, the proposed method scenario produces more oil at the end and indicated that the proposed method can be applied for better management and improvement, which is a signature of improvement in the CO_2 injection efficiency (Fig. 8).

Furthermore, gas production (Fig. 9) suddenly increases in all scenarios (this is the time when the CO_2 breakthrough has started). However, the breakthrough time in the proposed method has been delayed compared to the other scenarios. It means that the cross-section area obtained from the analytical method has helped the ICD

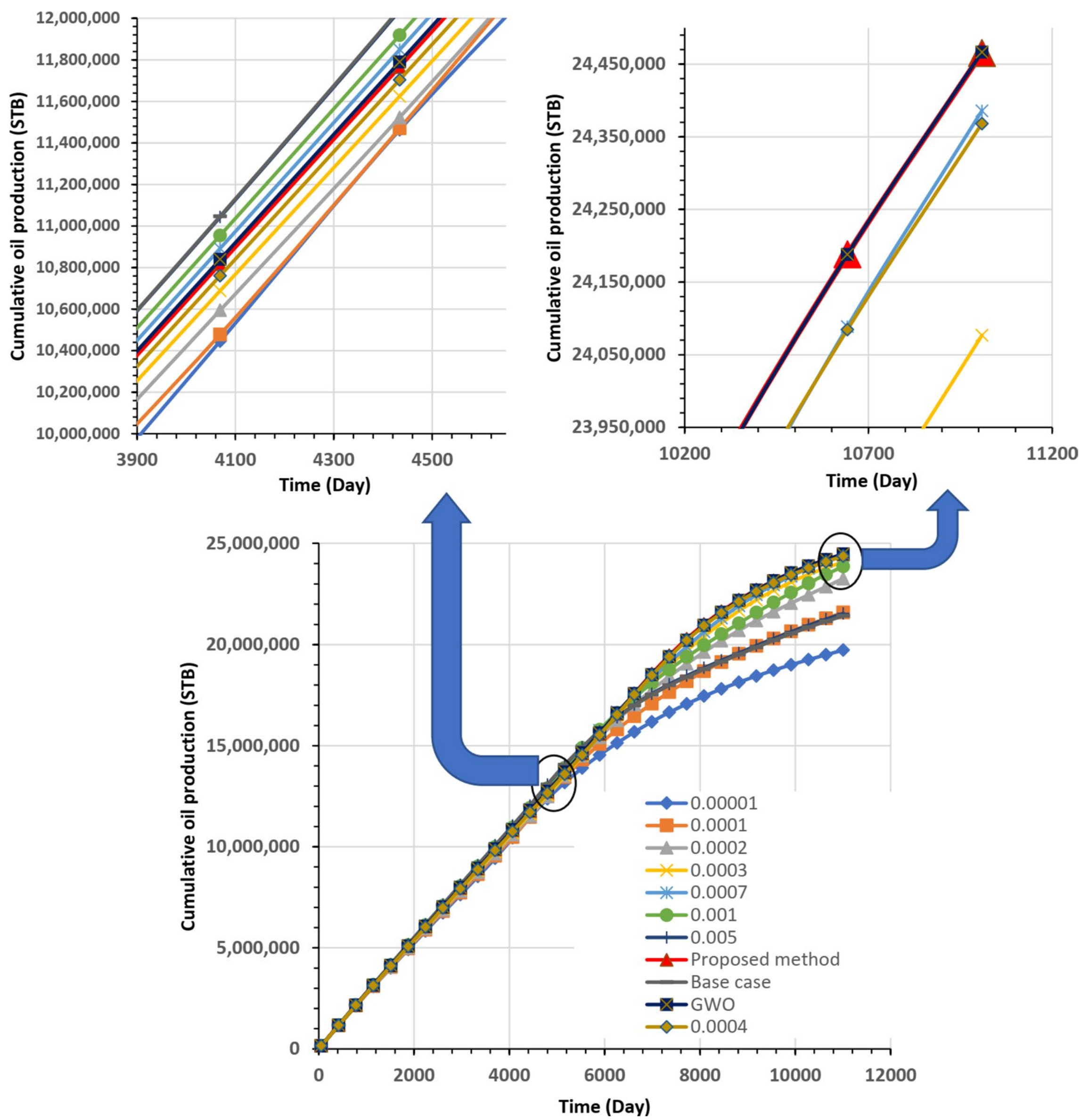

Fig. 7 Comparison of Cumulative oil production for all scenarios

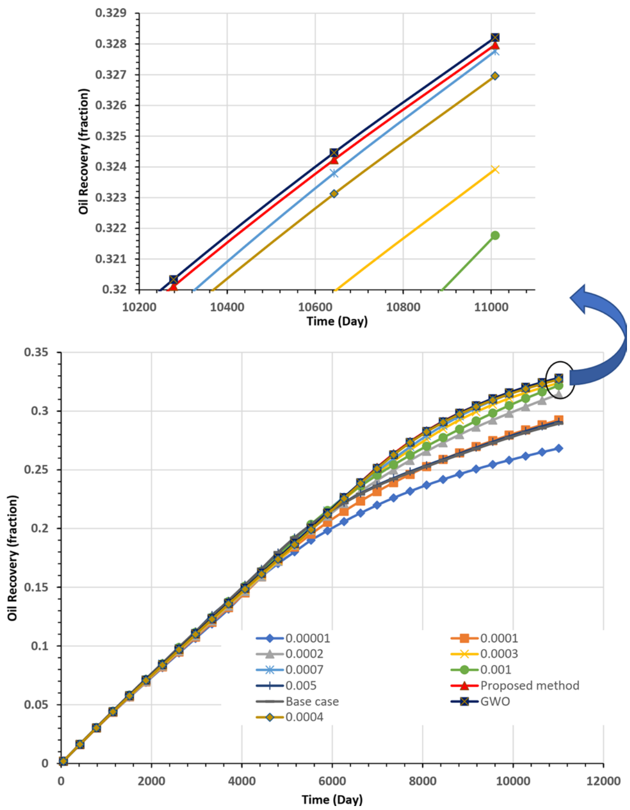

Fig. 8 Comparison of oil Recovery for all scenarios

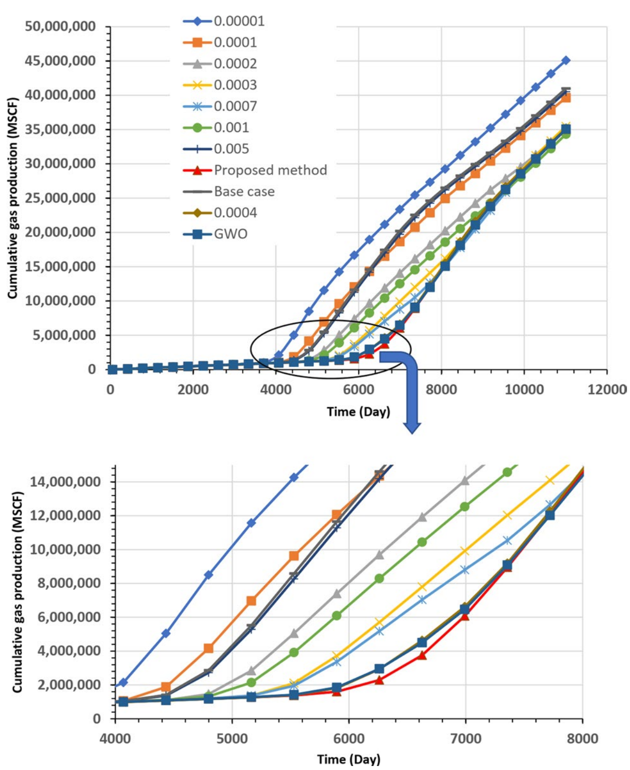

Fig. 9 Comparison of Cumulative Gas production for all scenarios

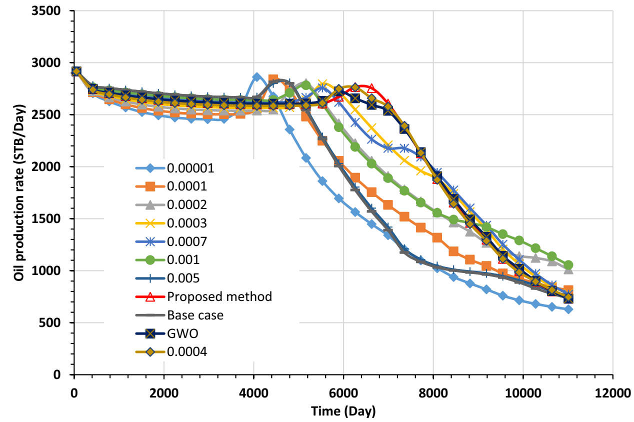

Fig. 10 Comparison of oil production Rate for all scenarios

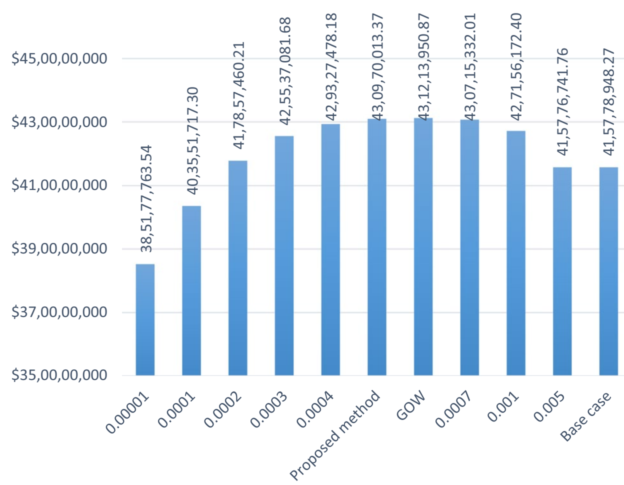

Fig. 11 NPV for all scenarios

perform much better than other methods in controlling breakthrough time and controlling gas production. Also, as shown in Fig. 10, the plateau period for the proposed method is longer than other scenarios due to the efficient CO_2 allocation in both layers and postponing CO_2 breakthrough time.

Finally, economic analysis performs to see how net present value can be improved by the proposed method compared to the other scenarios. The result shows that the proposed method has appropriate NPV between other scenarios – only GWO algorithm very slightly has a better NPV compared to the proposed method about 0.05 present (Fig. 11).

To sum up the results, the results of the simulation are shown great improvement in CO_2 flood performance after employing the proposed method and GWO scenario compare to the other scenarios. A better daily oil production profile was achieved and more cumulative oil was produced and gas production decreased. Also, there is a significant improvement in field oil efficiency after applying the new analytical approach for setting ICDs flow area. Also, gas breakthrough time was maximized as a result of employing the proposed method. Moreover, it should be noted that, although both the optimization method and the proposed method have better performance, GWO was time-consuming and needed more data.

Advantages and disadvantages

Although both the optimization method (GWO) and the proposed method have been able to control the fluid front movement in the two layers very well, but the advantage of the proposed method over the optimization is that, first the simulation model is not required for the proposed method and only reservoir layer properties and total injection rate is needed. Second, the desired valve opening can be obtained very fast with the given equation, while for optimization, complete information and all the details and complexity of the reservoir for simulation are required, and the calculation time is very long.

Summary and conclusions

- The utilization of the proposed method for setting inflow control devices flow area in the reservoir containing thief and high permeable zones assists in improving CO_2 flood performance not only by reducing gas production, but also by improving oil recovery and extending the production plateau period.
- The new analytical technique can effectively set an ICD flow area in keeping with its dynamic and petrophysical properties in order to delay and maximize CO_2 breakthrough time.
- The proposed method only requires reservoir layer properties and total rate of injection data, while all the details and complexity of the reservoir for simulation are needed for other methods, which are based on reservoir simulation.
- The ICD flow area can be obtained very fast with the given formula, while other methods, especially optimization algorithm is time-consuming.
- Utilizing the proposed formula for setting ICDs flow area for a cost-effective and efficient CO_2 injection in underground reservoirs is an application of the developed methodology for CCUS projects.
- The findings of the presented analytical formula can help researchers for a better understanding of parameters affecting ICD flow area such as reservoir permeability.

Funding The authors declare that they have no relevant financial or non-financial interests to disclose.

References

Aakre H, Mathiesen V, Moldestad B (2018) Performance of CO_2 flooding in a heterogeneous oil reservoir using autonomous inflow control. J Pet Sci Eng 167:654–663

Alhuthali AH, Datta-Gupta A, Yuen B, Fontanilla JP (2010) Field applications of waterflood optimization via optimal rate control with smart wells. SPE Reserv Eval Eng 13(03):406–422

Amar MN, Zeraibi N, Redouane K (2018) Bottom hole pressure estimation using hybridization neural networks and grey wolves optimization. Petroleum 4(4):419–429

Brouwer D, Jansen J, Van der Starre S, Van Kruijsdijk C, Berentsen C (2001) Recovery increase through water flooding with smart well technology. In: Paper presented at the SPE European Formation Damage Conference. https://doi.org/10.2118/68979-MS

Brouwer D, Nævdal G, Jansen J, Vefring EH, Van Kruijsdijk C (2004) Improved reservoir management through optimal control and continuous model updating. In: Paper presented at the SPE Annual Technical Conference and Exhibition. https://doi.org/10.2118/90149-MS

Cao J, Zhang N, Johansen TE (2019) Applications of fully coupled well/near-well modeling to reservoir heterogeneity and formation damage effects. J Pet Sci Eng 176:640–652

Chen B, Reynolds AC (2017) Optimal control of ICV's and well operating conditions for the water-alternating-gas injection process. J Pet Sci Eng 149:623–640

Dejam M, Hassanzadeh H (2018a) Diffusive leakage of brine from aquifers during CO2 geological storage. Adv Water Resour 111:36–57

Dejam M, Hassanzadeh H (2018b) The role of natural fractures of finite double-porosity aquifers on diffusive leakage of brine during geological storage of CO_2. Int J Greenh Gas Control 78:177–197

Fetkovich M (1975) Multipoint testing of gas wells. SPE Mid-Continent Section Continuing Education Course, Tulsa, OK

Fonseca R, Leeuwenburgh O, Rossa ED, Van den Hof PM, Jansen J-D (2015) Ensemble-based multi-objective optimization of on-off control devices under geological uncertainty. In: Paper presented at the SPE Reservoir Simulation Symposium. https://doi.org/10.2118/173268-PA

GeoQuest S (2014) ECLIPSE reference manual. Schlumberger, Houston

Hassanabadi M, Motahhari SM, Nadri Pari M (2012) Optimization of ICDs' port size in smart wells using particle swarm optimization (PSO) algorithm through neural network modeling. Nashrieh Shimi Va Mohandesi Shimi Iran 31(2):55–69

Li H, Zheng S, Yang D (2013) Enhanced swelling effect and viscosity reduction of solvent (s)/CO2/heavy-oil systems. SPE J 18(04):695–707

Mirjalili S, Mirjalili SM, Lewis A (2014) Grey wolf optimizer. Adv Eng Softw 69:46–61

Mohammadpourmarzbali S, Rafiei Y, Fahimpour J (2019) Improved waterflood performance by employing permanent down-dole control devices: Iran case study. In: Paper presented at the Youth Technical Sessions Proceedings: VI Youth Forum of the World Petroleum Council-Future Leaders Forum (WPF 2019), June 23–28, 2019, Saint Petersburg, Russian Federation. 333

Naus M, Dolle N, Jansen J-D (2004) Optimization of commingled production using infinitely variable inflow control valves. In: Paper presented at the SPE Annual Technical Conference and Exhibition. doi:https://doi.org/10.2118/90959-PA

Perera MSA, Gamage RP, Rathnaweera TD, Ranathunga AS, Koay A, Choi X (2016) A review of CO2-enhanced oil recovery with a simulated sensitivity analysis. Energies 9(7):481

Rahimbakhsh A, Rafiei Y (2018) Investigating the effect of employing inflow control devices on the injection well on the SAGD process efficiency using an integrated production modeling. In: Paper presented at the SPE EOR Conference at Oil and Gas West Asia. doi:https://doi.org/10.2118/190407-MS

Ratterman EE, Augustine JR, Voll BA (2005) New technology applications to increase oil recovery by creating uniform flow profiles in horizontal wells: case studies and technology overview. In: Paper presented at the International Petroleum Technology Conference. https://doi.org/10.2523/IPTC-10177-MS

Safaei-Farouji M, Thanh HV, Dai Z, Mehbodniya A, Rahimi M, Ashraf U, Radwan AE (2022a) Exploring the power of machine learning to predict carbon dioxide trapping efficiency in saline aquifers for carbon geological storage project. J Clean Prod 372:133778

Safaei-Farouji M, Thanh HV, Dashtgoli DS, Yasin Q, Radwan AE, Ashraf U, Lee K-K (2022b) Application of robust intelligent schemes for accurate modelling interfacial tension of CO_2 brine systems: implications for structural CO_2 trapping. Fuel 319:123821

Salvesen Holte S, Knutsen JVE, Sømme Ommedal R, Moldestad BM (2020) Simulation of enhanced oil recovery with CO_2 injection

Siqueira TA, Iglesias RS, Ketzer JM (2017) Carbon dioxide injection in carbonate reservoirs–a review of CO_2-water-rock interaction studies. Greenh Gases Sci Technol 7(5):802–816

Ugwu AA, Moldestad BM (2018) The application of inflow control device for an improved oil recovery using ECLIPSE. In: Paper presented at the Proceedings of The 9th EUROSIM Congress on Modelling and Simulation, EUROSIM 2016, The 57th SIMS Conference on Simulation and Modelling SIMS 2016. 694–699

Van Essen G, Jansen J-D, Brouwer D, Douma SG, Zandvliet M, Rollett KI, Harris D (2010) Optimization of smart wells in the St. Joseph field. SPE Reserv Eval Eng 13(04):588–595

Yang Z, Li X, Li D, Yin T, Zhang P, Dong Z, Lin M, Zhang J (2019) New method based on CO_2-Switchable wormlike micelles for controlling CO_2 breakthrough in a tight fractured oil reservoir. Energy Fuels 33(6):4806–4815

Yu W, Lashgari H, Sepehrnoori K (2014) Simulation study of CO2 huff-n-puff process in Bakken tight oil reservoirs. In: Paper presented at the SPE Western North American and Rocky Mountain Joint Meeting. https://doi.org/10.2118/169575-MS

Zhang L, Ren B, Huang H, Li Y, Ren S, Chen G, Zhang H (2015) CO_2 EOR and storage in Jilin oilfield China: monitoring program and preliminary results. J Petrol Sci Eng 125:1–12

Zhang Y, Yu W, Li Z, Sepehrnoori K (2018) Simulation study of factors affecting CO_2 Huff-n-Puff process in tight oil reservoirs. J Pet Sci Eng 163:264–269

Publisher's Note Springer Nature remains neutral with regard to jurisdictional claims in published maps and institutional affiliations.